Liquid Crystals
Publication details, including instructions for authors and subscription information:
http://www.informaworld.com/smpp/title~content=t713926090

Field Effects in Nematic Liquid Crystals in Terms of Catastrophe Theory

G. Derfel[a]
[a] Institute of Physics, Technical University of Łódź, Łódź, Poland

To cite this Article Derfel, G.(1988) 'Field Effects in Nematic Liquid Crystals in Terms of Catastrophe Theory', Liquid Crystals, 3: 10, 1411 — 1424
To link to this Article: DOI: 10.1080/02678298808086621
URL: http://dx.doi.org/10.1080/02678298808086621

LIQUID CRYSTALS, 1988, VOL. 3, NO. 10, 1411–1424

Field effects in nematic liquid crystals in terms of catastrophe theory

by G. DERFEL
Institute of Physics, Technical University of Łódź, 93-005 Łódź, Poland

(*Received 4 June 1987; accepted 17 February 1988*)

The field effects in nematic liquid crystal layers are reanalysed using catastrophe theory. The layer with pretilted director orientation and obliquely applied magnetic field, the hybrid aligned nematic cell and twisted nematic structures are considered. The stable solutions are identified and transitions between them are specified. The results are in essential agreement with previous work. Some details concerning the behaviour near the threshold are revealed.

1. Introduction

The influence of external fields on liquid crystal layers is usually described by means of the Euler–Lagrange equations. The solutions, which are obtained typically by numerical methods, provide detailed quantitative information on the director distribution at any field strength. The calculations sometimes give several solutions under the same conditions, which are related to different values of the free energy of the layer. The aim of this paper is to apply the methods developed by catastrophe theory to resolving the problem of the stability of such solutions.

Catastrophe theory, originated by Thom [1], is topological in nature. It stems from the theory of singularities of smooth mappings and from the theory of bifurcations of dynamical systems. According to Thom's theorem, any family of smooth functions of n variables and r parameters is equivalent to one of a few archetypal forms. All but two of them involve a dependence on parameters and are called the catastrophes. This name reflects the fact that a smooth change of parameters can induce abrupt changes in the topological character of the function. The catastrophe predicts the number and kind of extremes of the considered function for any set of parameters, and the influence of the parameter variation on the disposition of the extremes. Seven elementary catastrophes result if $r \leqslant 4$. (See [2] for a review.) In this paper, two of them will be applied. If $n = 1$ (one behaviour factor) and $r = 2$ (two control factors), the cusp catastrophe is encountered. This is the most productive catastrophe, suitable for the description of many physical systems [3]. It is easily recognizable and has a straightforward three dimensional representation. It was applied by Vasilyev [4] to the case of the pure twist deformation of the nematic layer in a magnetic field. Another catastrophe, called the butterfly, results if $r = 4$. Both of them belong to the same class of cuspoidal catastrophes and are described in the next section. In §3, the cusp is applied to the case of the pretilted nematic slab in oblique magnetic field. The hybrid aligned cell is considered in §4. It is found that there is no reason for a catastrophic behaviour. In §5, the twisted and supertwisted nematic cells are treated by means of the butterfly. Section 6 is devoted to a short discussion of the approach applied.

In all cases the static deformations occurring in a magnetic field are taken into account. The magnetic field is chosen for the sake of simplicity as the relative

diamagnetic anisotropy $\beta = \chi_a/\chi_\perp$ is small and only terms linear in β are important. The electric field is considered only for twisted structures.

The qualitative features obtained by application of catastrophe theory are valid whereas the quantitative results are only approximate.

2. The cusp and the butterfly catastrophes

The standard form of the cusp catastrophe is

$$f = x^4/4 + ax^2/2 + bx, \tag{1}$$

where x is a variable, a and b are parameters. The extremes of this function are given by

$$x^3 + ax + b = 0. \tag{2}$$

This yields the equation of the catastrophe manifold which is a surface in a, b and x coordinates, called the behaviour surface. Its shape is shown in figure 1. This surface possesses two folds for $a < 0$. The projection of the folds onto the ab plane (control plane) is the semicubical parabola

$$4a^3 + 27b^2 = 0. \tag{3}$$

It forms the bifurcation set of the catastrophe given by the set of solutions of the equations

$$\left.\begin{aligned} \partial f/\partial x &= 0, \\ \partial^2 f/\partial x^2 &= 0. \end{aligned}\right\} \tag{4}$$

There is one singular point (0, 0) on the control plane, whereas the behaviour surface is smooth. There are three sheets of the behaviour surface between the branches of the curve, corresponding to three different real roots of equation (2), two minima and one maximum. Only one minimum is retained exactly on the line (3). The other merges with the maximum and the inflection point arises. Outside the bifurcation set there is only one sheet due to one minimum.

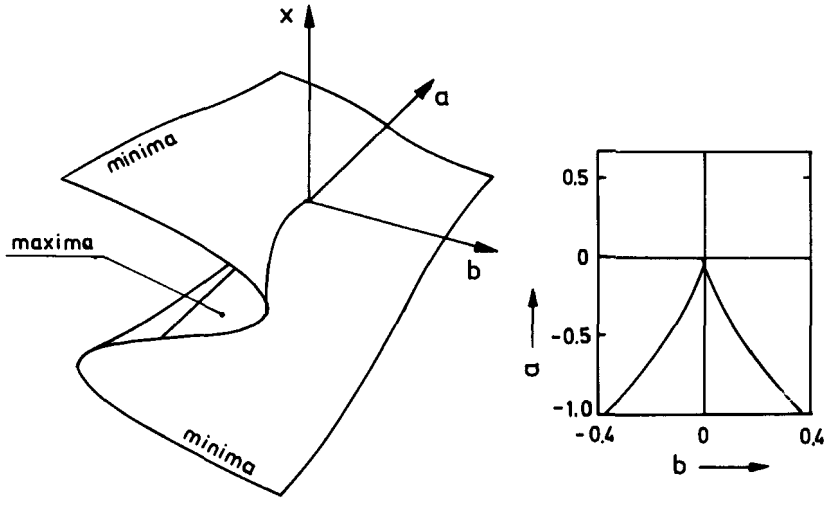

Figure 1. The geometry of the cusp catastrophe and its bifurcation set.

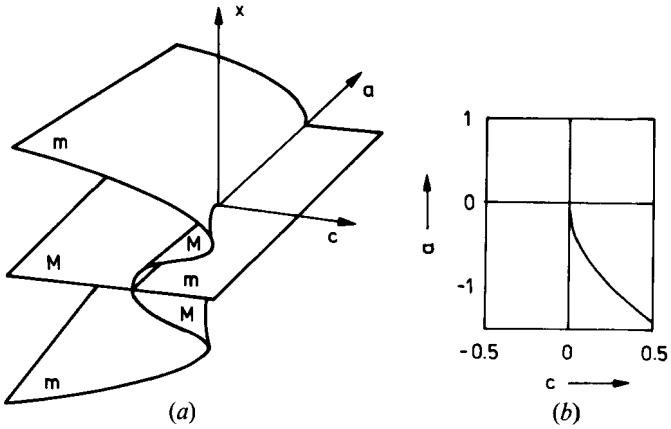

(*a*) (*b*)

Figure 2. The cross section of the behaviour manifold of the buterfly catastrophe for $b = d = 0$, (*a*) and the corresponding bifurcation set, (*b*) (*M*—maxima, *m*—minima).

The butterfly catastrophe results from a function of the type

$$f = x^6/6 + ax^4/4 + bx^3/3 + cx^2/2 + dx. \tag{5}$$

Its extremes are given by the condition

$$x^5 + ax^3 + bx^2 + cx + d = 0 \tag{6}$$

which yields the equation of the catastrophe manifold in five dimensions. As the dimension of the control space is four, it is convenient to work with two dimensional sections of it. The control space reduces then to the plane and the behaviour surface is easy to draw. Figure 2(*a*) presents its shape for $b = d = 0$ and figure 2(*b*) gives the section of the bifurcation set. It consists of the line $c = 0$ and one branch of the parabola $c = a^2/4$ for $a < 0$. There are three regions of control plane characterized by a different number of extremes: (1) three minima, two maxima, (2) one maximum, two minima and (3) one minimum. There are five sheets of the behaviour surface overlying each other in the first case, three in the second and one in the last, corresponding to the real roots of equation (6).

If the potential energy of the system has the form (1) or (5), we can make use of the diagram, like that shown in figures 1 or 2, and find the character of the equilibrium states and their evolution during variation of parameters. This approach is applied in the following sections.

3. Pretilted nematic layer

The geometry of the system considered in this section is shown in figure 3. This configuration was studied by Onnagawa and Miyashita [5] in the usual manner. The director is aligned in one direction with a preliminary tilt θ_0 on both container surfaces. The magnetic field of strength H is applied at an angle α to the normal to the layer. The free energy density in this case is given by

$$g = (k_3/2)\,[1 - K\cos^2(\theta_0 + \xi)](d\xi/dz)^2 - (1/2)\chi_a H^2 \sin^2(\theta_0 + \xi - \alpha), \tag{7}$$

where $\xi(z) = \theta(z) - \theta_0$, and $\theta(z)$ denotes the angle between the distorted director and the plates; $K = 1 - k_1/k_3$, k_1 and k_3 are splay and bend elastic constants,

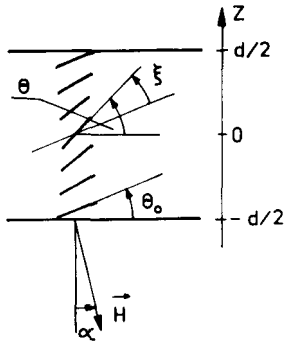

Figure 3. The definition of the angles describing the geometry of the nematic layer.

respectively, and χ_a is the diamagnetic susceptibility anisotropy. If small deformations are assumed, only the first term in the Fourier expansion of $\xi_m(z)$ is significant; namely

$$\xi(z) = \xi_m \cos(\pi z/d), \tag{8}$$

where ξ_m is the maximum value in the mid-plane of the layer.

Using equations (7) and (8) we can calculate the free energy per unit area of the layer, G. For this purpose the free energy density is first expanded in a Taylor series of ξ_m in the vicinity of $\xi_m = 0$, and then integrated. The resulting expression has the form

$$G = a_0 + a_1\xi_m + a_2\xi_m^2 + a_3\xi_m^3 + a_4\xi_m^4 + O(5), \tag{9}$$

where

$$\left.\begin{aligned} a_1 &= -(\pi k_3 h/d)\sin[2(\theta - \alpha)], \\ a_2 &= (\pi^2 k_3/4d)\{1 - K\cos^2\theta_0 - h\cos[2(\theta - \alpha)]\}, \\ a_3 &= (\pi k_3/3d)\{K\sin 2\theta_0 + (4h/3)\sin[2(\theta_0 - \alpha)]\}, \\ a_4 &= (\pi^2 k_3/16d)\{K\cos 2\theta_0 + h\cos[2(\theta_0 - \alpha)]\}, \end{aligned}\right\} \tag{10}$$

$h = (H/H_b)^2$ and $H_b = (\pi/d)(k_3/\chi_a)^{1/2}$. Only the reduced quantities K and h are necessary to compute ξ_m, therefore the following results are valid for arbitrary k_3 and d. The term a_0 is unimportant, as it can be removed by a suitable choice of zero energy level. It is evident, that if $\theta_0 = 0$, $\alpha = 0$ and $h = 1 - K$, then the coefficients, a_1, a_2 and a_3 are zero, whereas $a_4 \neq 0$. According to the theorems of catastrophe theory, terms of order higher than four in equation (9) can be disregarded. Following the rules for the classification of functions into the forms of catastrophes systematized in [6], a new variable is introduced:

$$x = (4|a_4|)^{1/4}(\xi_m + a_3/4a_4). \tag{11}$$

The energy G, truncated in this way can be written in the form of the cusp catastrophe (1), in which

$$a = (8a_2a_4 - 3a_3^2)/8a_4|a_4|^{1/2}, \tag{12}$$

$$b = (16a_1a_4^2 + 2a_3^3 - 8a_2a_3a_4)/(4|a_4|)^{5/4}. \tag{13}$$

The behaviour of the director in the layer can be analysed by variation of the parameters α, θ_0, K or h. Each set of parameters defines the point (a, b) on the control plane and the corresponding values of ξ_m. In the following some particular situations are described. In every case, one of the parameters is varied while the others are fixed. As a consequence of this, a trajectory in control plane is obtained which determines the solution of the problem. The figures show only the essential parts of the trajectories and everywhere $a_4 > 0$. However the trajectories may often have rather complicated shapes and spread far from the apex (0, 0).

For some particular ranges of the parameters, a_4 may be negative and the dual cusp catastrophe results. Its behaviour surface has the same shape as the ordinary cusp. The directions of the a and b axes are, however, reversed and hence the middle sheet represents stable equilibria, while the upper and lower sheets represent unstable equilibria. If $a_4 = 0$, the expansion of G is limited to third degree and the solutions of the resulting quadratic equation fit the solutions obtained for $a_4 \neq 0$.

3.1. $\alpha = \theta_0$

This case was considered by Yamada [7]. Here the deformations of the layer are found for the variable magnetic field parameter h. Examples of the trajectories are shown in figure 4a, where the arrows indicate an increase of h.

For $\alpha = \theta_0 = 0$ or $\alpha = \theta_0 = \pi/2$, the splay or bend deformations, respectively, are obtained. Since $b = 0$, the trajectories run along the a axis. Figure 4(b) shows the maximum distorsion angle ξ_m versus the reduced magnetic field H/H_b. For $a > 0$, the only minimum is $\xi_m = 0$. The threshold magnetic field is reached and two non-zero, stable solutions appear in turn for $a = 0$. The threshold is given by $h_c = 1 - K\cos^2\theta_0$ and takes the well-known values $H_s = (\pi/d)(k_1/\chi_a)^{1/2}$ and $H_b = (\pi/d)(k_3/\chi_a)^{1/2}$.

If $\alpha = \theta_0 > 0$ the trajectory has two common points with the bifurcation set: the point of intersection and the point of tangence. For the magnetic field increasing from zero the solution is due to the upper sheet of the behaviour surface: $\xi_m = 0$. If

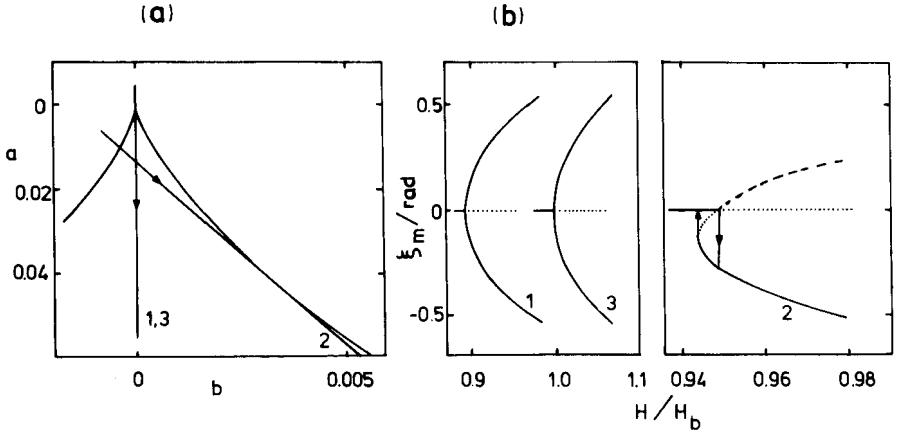

Figure 4. The trajectories (a) and the maximum distortion angle ξ_m versus the reduced magnetic field H/H_b (b). $K = 0{\cdot}2$. 1: $\alpha = \theta_0 = 0$, 2: $\alpha = \theta_0 = \pi/4$, 3: $\alpha = \theta_0 = \pi/2$. The arrows in ($a$) indicate the increase of the field strength. Full line—minima, dotted line —maxima, dashed line—unavailable minima.

the field reaches the value corresponding to the tangential point: $h = 1 - K\cos^2\theta_0$, i.e. $H = H_b(1 - K\cos^2\theta_0)^{1/2}$, ξ_m jumps to a value due to the lower sheet. If the magnetic field decreases, the jump takes place at the point of intersection and moves the solution back to the upper sheet, as shown in figure 4(*b*). The transition is therefore discontinuous and hysteresis appears. The opposite sign of ξ_m and the reverse direction of the jumps take place for $\alpha = \theta < 0$. The trajectories due to both cases are symmetrical with respect to the *a* axis.

3.2. $\alpha \neq \theta_0$

This case was studied by use of the variational method by Motooka and Fukuhara [8]. The trajectories determined by the variable field paremter h are shown in figure 5(*a*). Their shape is the same as for $\alpha = \theta_0$, but they are shifted to the left if $\alpha < \theta_0$ and to the right if $\alpha > \theta_0$. The $\xi_m(H/H_b)$ dependence is plotted in figure 5(*b*). In general there is no threshold in this case, but if α exceeds θ_0 by a sufficiently small value, the shift to the right is also very small and the trajectory intersects the bifurcation set in three points. Considerable deformation results at point *A* and decays at point *B*. The function $\xi_m(H/H_b)$ has an *S* shape and a small hysteresis also exists.

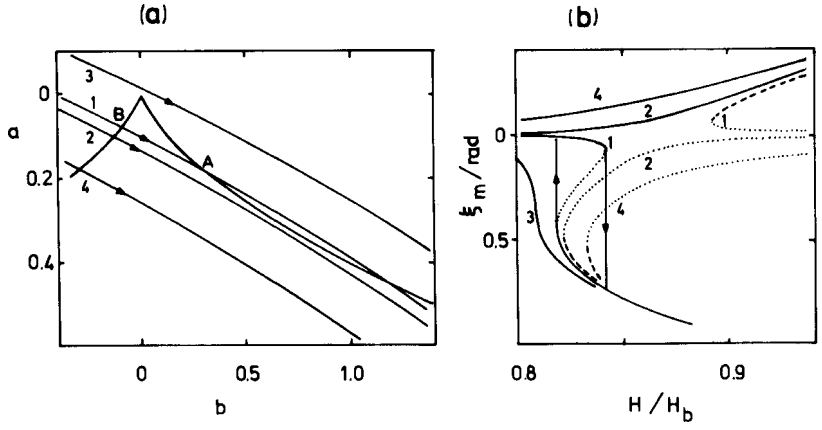

Figure 5. The trajectories (*a*) and the $\xi_m(H/H_b)$ dependence (*b*) for $\alpha \neq \theta_0$. $K = 0{\cdot}5$, $\theta_0 = 0{\cdot}25\pi$. 1: $\alpha = 0{\cdot}2505\pi$, 2: $\alpha = 0{\cdot}2495\pi$, 3: $\alpha = 0{\cdot}254\pi$, 4: $\alpha = 0{\cdot}246\pi$. In case 1, the considerable deformation results at point *A* and decays at point *B*.

Two particular situations in the case $\alpha \neq \theta_0$ can be distinguished:

$$\alpha = 0, \theta_0 \neq 0.$$

The magnetic field is applied normal to the layer of the pretilted nematic. The trajectory is, in its essential part, almost parallel to the *a* axis. There is no threshold (see figure 6(*a*), (*b*), trajectory 1).

$$\alpha \neq 0, \theta_0 = 0.$$

The planar nematic layer is under the influence of the oblique magnetic field. The trajectory 2 in figure 6(*a*) defined by the variable h gives the solution analogous to the

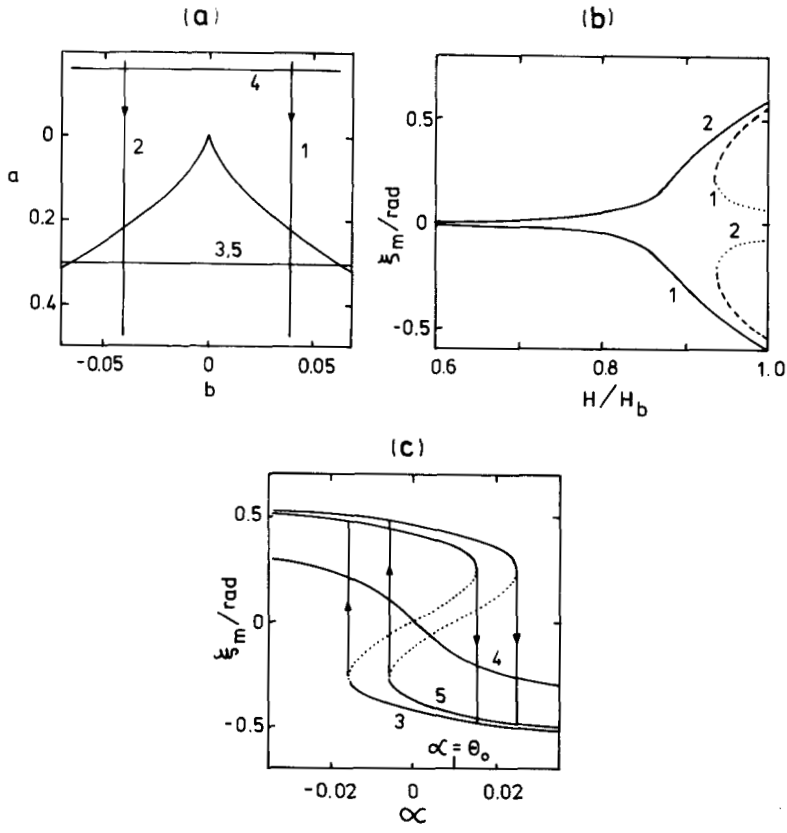

Figure 6. The trajectories (*a*), the $\xi_m(H/H_b)$ dependence (*b*) and the $\xi_m(\alpha)$ dependence (*c*) for $\alpha \neq \theta_0$. $K = 0{\cdot}2$. 1: $\theta_0 = -0{\cdot}01$, $\alpha = 0$, 2: $\theta_0 = 0$, $\alpha = -0{\cdot}01$, 3: $\theta_0 = 0$, $h = 0{\cdot}9$, 4: $\theta_0 = 0$, $h = 0{\cdot}75$, 5: $\theta_0 = 0{\cdot}01$, $h = 0{\cdot}9$.

preceding case shown in figure 6 (*b*). Trajectories 3, 4 and 5 for constant h and variable α are approximately parallel to the b axis. If $H > H_s$, they intersect the bifurcation set at two points. In figure 6 (*c*), the dependence of ξ_m on the magnetic field direction α is shown, hysteresis phenomena are evidently present. Figure 6 (*c*) presents only the central parts of the $\xi_m(\alpha)$ plot. If α tends to $\pm\pi/2$, $|\xi_m|$ reaches a maximum and then decays to zero. The centre of symmetry of the hysteresis curve is placed at $\alpha = \theta_0$.

4. Hybrid aligned nematic cell

In this case the director distribution is described by the angle $\theta(z)$. The orientation is planar at one plate and homeotropic at the other: $\theta_0(-d/2) = 0$; $\theta_0(d/2) = \pi/2$. If the one-constant approximation is assumed: $k_1 = k_2 = k_3 = k$, the analytical expression for the function $\theta(z)$ is obtained as

$$\theta(z) = (\pi z)/(2d) + \pi/4. \tag{14}$$

The energy of the layer deformed by a normal magnetic field is expanded in powers

of ξ_m. The expansion coefficients are:

$$\left.\begin{aligned} a_1 &= \pi^2 h/4, \\ a_2 &= \pi^2/4, \\ a_3 &= -\pi^2 h/8, \\ a_4 &= 0, \end{aligned}\right\} \tag{15}$$

where $h = (H/H_c)^2$, $H_c = (\pi/d)(k/\chi_\alpha)^{1/2}$. The second derivative of G, a_2, is always non-zero. The critical point is therefore non-degenerate and no catastrophe occurs. The expansion can be limited to second order and we can calculate the approximate solution for ξ_m:

$$\xi_m = -h/2. \tag{16}$$

In agreement with [9], the deformation increases with the square of magnetic field intensity.

5. Twisted nematic structures

In this section, the general geometry of the twisted structure, commonly employed in liquid crystal displays, is considered. The director is tilted in the same sense at both boundary plates, which are parallel to the xy plane. The preferred directions on the plates do not coincide. The twist angle ϕ between them and the tilt angle θ_0 can take arbitrary values. Initially the angle ω between the yz plane and the projection of the director onto the xy plane changes linearly with z from $-\phi/2$ to $\phi/2$. The magnetic field is applied perpendicular to the layer. The chirality of the nematic material is introduced and is measured by $q = \pi/\lambda$, where λ denotes the half of the pitch of the undistorted bulk material. Small deformations are assumed. Two angles are needed to characterize them: $\xi(z)$, defined by equation (8), and $\psi(z)$ which measures the field-induced rotation of director around the z axis. For symmetry reasons, $\psi(0) = 0$ and

$$\omega = \phi z/d + \psi_m \sin(2\pi z/d). \tag{17}$$

The free energy density in this case becomes a rather complicated expression

$$\begin{aligned} g = (1/2)\{&[(k_1 \cos^2\theta + k_3 \sin^2\theta)(\partial\theta/\partial z)^2 + \cos^2\theta(k_2 \cos^2\theta + k_3 \sin^2\theta)(\partial\omega/\partial z)^2] \\ &- \chi_\alpha H^2 \sin^2\theta + 2k_2 q \cos^2\theta(\partial\omega/\partial z)\}. \end{aligned} \tag{18}$$

Expansion of equation (18) in a Taylor series in ξ_m and ψ_m followed by integration gives the total energy per unit area of the slab in the form

$$\begin{aligned} G = {} & a_0 + a_1\xi_m + a_2\xi_m^2 + a_3\xi_m^3 + a_4\xi_m^4 + a_5\xi_m^5 + a_6\xi_m^6 + \cdots + b_1\psi_m\xi_m + b_2\psi_m\xi_m^2 \\ & + b_3\psi_m\xi_m^3 + b_4\psi_m\xi_m^4 + b_5\psi_m\xi_m^5 + \cdots + c_0\psi_m^2 + c_1\psi_m^2\xi_m + c_2\psi_m^2\xi_m^2 \\ & + c_3\psi_m^2\xi_m^3 + c_4\psi_m^2\xi_m^4 + \ldots. \end{aligned} \tag{19}$$

The angle ψ_m appears in this expansion only to first and second degree. By use of the algorithm given in [6], this expansion can be transformed into the normalized form, in which the essential variable is separated from the inessential one. It turns out that ξ_m is essential and hence G is equivalent to the sum of a power series in ξ_m and of

a second order term in a new inessential variable y (an unimportant constant is omitted):

$$G_1 = a_1\xi_m + a_2\xi_m^2 + a_3\xi_m^3 + a_4'\xi_m^4 + a_5\xi_m^5 + a_6'\xi_m^6 + \cdots + c_0 y^2 \qquad (20)$$

with

$$\left.\begin{aligned}
a_1 &= (\pi k_1/d)\sin 2\theta_0\{-h - 2k_t(d/\lambda)(\phi/\pi) \\
&\quad + (\phi/\pi)^2[(k_b - 2k_t)\cos^2\theta_0 - k_b\sin^2\theta_0]\}, \\
a_2 &= (\pi^2 k_1/4d)\{\cos^2\theta_0 + k_b\sin^2\theta_0 - h\cos 2\theta_0 - 2k_t(d/\lambda)(\phi/\pi)\cos 2\theta_0 \\
&\quad + (\phi/\pi)^2[(k_b - 2k_t)\cos^4\theta_0 + k_b\sin^4\theta_0 - 1{\cdot}5(k_b - k_t)\sin^2 2\theta_0]\}, \\
a_3 &= (4\pi k_1/9d)\sin 2\theta_0\{0{\cdot}75(k_b - 1) + h + 2k_t(d/\lambda)(\phi/\pi) \\
&\quad + (\phi/\pi)^2[(5k_t - 4k_b)\cos^2\theta_0 + (4k_b - 3k_t)\sin^2\theta_0]\}, \\
a_4 &= (\pi^2 k_1/16d)\{(k_b - 1)\cos 2\theta_0 + h\cos 2\theta_0 + 2k_t(d/\lambda)(\phi/\pi)\cos 2\theta_0 \\
&\quad + (\phi/\pi)^2[(5k_t - 4k_b)\cos^4\theta_0 - (4k_b - 3k_t)\sin^4\theta_0 \\
&\quad + 6(k_b - k_t)\sin^2 2\theta_0]\}, \\
a_5 &= (16\pi k_1/225d)\sin 2\theta_0\{1{\cdot}25(1 - k_b) - h - 2k_t(d/\lambda)(\phi/\pi) \\
&\quad + (\phi/\pi)^2[(16k_b - 17k_t)\cos^2\theta_0 - (16k_b - 15k_t)\sin^2 2\theta_0]\}, \\
a_6 &= (\pi^2 k_1/144d)\{1{\cdot}5(1 - k_b)\cos 2\theta_0 - h\cos 2\theta_0 - 2k(d/\lambda)(\phi/\pi)\cos 2\theta_0 \\
&\quad + (\phi/\pi)^2[(16k_b - 17k_t)\cos^4\theta_0 + (16k_b - 15k_t)\sin^4\theta_0 \\
&\quad - 24(k_b - k_t)\sin^2 2\theta_0]\}.
\end{aligned}\right\} \qquad (21)$$

$$\left.\begin{aligned}
b_2 &= (\pi^2 k_1/2d)\{(\phi/\pi)[(k_b - 2k_t)\cos^4\theta_0 + k_b\sin^4\theta_0 \\
&\quad - 1{\cdot}5(k_b - k_t)\sin^2 2\theta_0] - k_t(d/\lambda)\cos 2\theta_0\}, \\
b_4 &= (\pi^2 k_1/6d)\{(\phi/\pi)[(5k_t - 4k_b)\cos^4\theta_0 - (4k_b - 3k_t)\sin^4\theta_0 \\
&\quad + 6(k_b - k_t)\sin^2 2\theta_0] + k_t(d/\lambda)\cos 2\theta_0\}, \\
c_0 &= (\pi^2 k_1/d)(k_t\cos 2\theta_0 + k_b\sin^2\theta_0)\cos^2\theta_0, \\
c_2 &= (\pi^2 k_1/2d)[(k_b - 2k_t)\cos^4\theta_0 + k_b\sin^4\theta_0 - 1{\cdot}5(k_b - k_t)\sin^2 2\theta_0],
\end{aligned}\right\} \qquad (22)$$

$$\left.\begin{aligned}
a_4' &= a_4 - b_2^2/4c_0, \\
a_6' &= a_6 - b_2 b_4/2c_0 + b_2^2 c_2/4c_0^2, \\
y &= (b_2/2c_0)\xi_m^2 + [(2c_0 b_4 - c_2 b_2)/4c_0^2]\xi_m^4 + (b_2 c_4/4c_0^2)\xi_m^6 \\
&\quad + \psi_m[1 + (c_2/2c_0)\xi_m^2 + (c_4/2c_0)\xi_m^4],
\end{aligned}\right\} \qquad (23)$$

and

$$k_t = k_2/k_1,\ k_b = k_3/k_1.$$

These coefficients depend on several system parameters namely θ_0, k_b, k_t, d/λ, ϕ, and h. It is possible to find some relations between them, which cause the coefficients a_1, a_2, a_3, a_4', a_5 to vanish. Indeed, if $\theta_0 = 0$, $h = h_c = 1 + (\phi/\pi)^2(k_b - 2k_t) - 2k_t(d/\lambda)(\phi/\pi)$, and

$$\begin{aligned}\phi/\pi = \{&(s-2)(d/\lambda) \pm \{(d/\lambda)^2(s-2)^2 \\ &+ (s^2 - s + 1)[s - (d/\lambda)^2]\}^{1/2}\}/(s^2 - s + 1),\end{aligned} \tag{24}$$

where $s = k_b/k_t$, the first non-zero coefficient is a_6'. The expansion may be limited therefore, to the sixth degree, and, by use of the new variable

$$x = (6|a_6'|)^{1/6}(\xi_m + a_5/6a_6') \tag{25}$$

transformed into the standard form of the butterfly catastrophe (5). (In the cases considered in §3, the coefficient a_4 cannot vanish together with a_1, a_2 and a_3 and so gives rise to the cusp catastrophe.) The control parameters are given by

$$\left.\begin{aligned} a &= (12a_4'a_6' - 5a_5^2)/3a_6'(6|a_6'|)^{2/3}, \\ b &= (5a_5^3 - 18a_4'a_5a_6' + 27a_3a_6'^2)/9a_6'^2(6|a_6'|)^{1/2}, \\ c &= (-5a_5^4 - 24a_4'a_5^2a_6' - 72a_3a_5a_6'^2 + 144a_2a_6'^3)/72a_6'^3(6|a_6'|)^{1/3}, \\ d &= (a_5^5 - 6a_4'a_5^3a_6' + 27a_3a_5^2a_6'^2 - 108a_2a_5a_6'^3 + 324a_1a_6'^4)/324a_6'^4(6|a_6'|)^{1/6}. \end{aligned}\right\} \tag{26}$$

The values of ξ_m and ψ_m can be derived from the minimalization conditions. In particular from $\partial G/\partial\psi_m = 0$ we obtain

$$\begin{aligned}\psi_m = &-(b_1\xi_m + b_2\xi_m^2 + b_3\xi_m^3 + b_4\xi_m^4 + b_5\xi_m^5)/2(c_0 + c_1\xi_m \\ &+ c_2\xi_m^2 + c_3\xi_m^3 + c_4\xi_m^4),\end{aligned} \tag{27}$$

where

$$\begin{aligned} b_1 &= (4\pi k_1/3d)\sin 2\theta_0\{(\phi/\pi)[(k_b - 2k_t)\cos^2\theta_0 - k_b\sin^2\theta_0] - k_t(d/\lambda)\}, \\ b_3 &= (16\pi k_1/15d)\sin 2\theta_0\{(\phi/\pi)[(5k_t - 4k_b)\cos^2\theta_0 + (4k_b - 3k_t)\sin^2\theta_0] \\ &\quad + k_t(d/\lambda)\}, \\ b_5 &= (64\pi k_1/315d)\sin 2\theta_0\{(\phi/\pi)[(16k_b - 17k_t)\cos^2\theta_0 + (16k_b - 15k_t)\sin^2\theta_0] \\ &\quad - k_t(d/\lambda)\}, \\ c_1 &= (28\pi k_1/15d)\sin 2\theta_0[(k_b - 2k_t)\cos^2\theta_0 - k_b\sin^2\theta_0], \\ c_3 &= (304\pi k_1/315d)\sin 2\theta_0[(5k_t - 4k_b)\cos^2\theta_0 + (4k_b - 3k_t)\sin^2\theta_0], \\ c_4 &= (7\pi^2 k_1/48d)[(5k_t - 4k_b)\cos\theta_0 - (4k_b - 3k_t)\sin^4\theta_0 + 6(k_b - k_t)\sin^2 2\theta_0]. \end{aligned}$$

In the following, the angles ξ_m and ψ_m are presented as a function of the reduced magnetic field in several distinct cases.

5.1. $\theta_0 = 0$

Zero tilt offers a significant simplification of the problem. Since $b = d = 0$, it is easy to draw the trajectories on the control plane ac. In figure 7 (*a*) some examples of

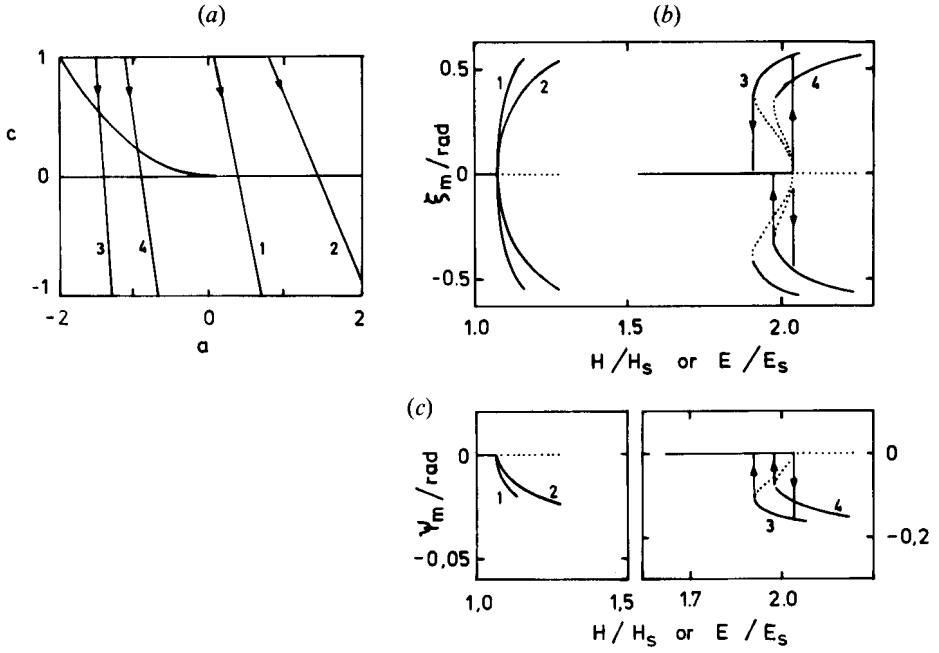

Figure 7. The trajectories (*a*), the deformation angles ξ_m (*b*), and ψ_m (*c*) as a function of the reduced field for the twisted structures. $k_b = 1{\cdot}4$, $k_t = 0{\cdot}4$, $\theta_0 = 0$. 1: $\phi = \pi/2$, $d/\lambda = 0$, $\gamma = 0$, 2: $\phi = \pi/2$, $d/\lambda = 0$, $\gamma = 1$, 3: $\phi = 1{\cdot}5\pi$, $d/\lambda = -1{\cdot}5$, $\gamma = 0$, 4: $\phi = 1{\cdot}5\pi$, $d/\lambda = -1{\cdot}5$, $\gamma = 1$.

trajectories are shown. They start in the region, where one minimum $x = 0$ ($\xi_m = 0$) exists. The director distribution remains undistorted until the line $c = 0$ is achieved which defines the threshold field

$$h_c = 1 + (\phi/\pi)^2(k_b - 2k_t) - 2k_t(d/\lambda)(\phi/\pi). \tag{28}$$

Above this threshold, there are two symmetrical minima and one maximum. Under certain circumstances the trajectory intersects the branch of the parabola $c = a^2/4$ and runs across the region with five extremes. Their values can be obtained from equation (6),

$$x_1 = 0, \tag{29}$$

$$x_{2,3,4,5} = \pm\{[-a \pm (a^2 - 4c)^{1/2}]/2\}^{1/2}. \tag{30}$$

For the field increasing from zero, the only solution $\xi_m = 0$ is due to the middle, flat sheet of the behaviour surface. At the threshold, ξ_m jumps to one of the two values corresponding to the exterior sheets. If the field decreases, the jump occurs when the trajectory meets the parabola and the deformation disappears, in consequence hysteresis takes place.

The hysteresis of $\xi_m(H/H_s)$ dependence is the most characteristic phenomenon in the behaviour of the systems considered. It occurs if the threshold $c = 0$ is achieved at $a < 0$. This gives the condition

$$\phi/\pi \gtrless \{(s-2)(d/\lambda) \pm \{(d/\lambda)^2(s-2)^2 + (s^2 - s + 1) \times [s - (d/\lambda)^2]\}^{1/2}\}/(s^2 - s + 1), \tag{31}$$

for hysteresis. For $\phi = \pi/2$ and $d/\lambda = 0$, it is identical with the inequality given by Leslie, [10]: $k_b/k_t > 4{\cdot}792$.

For liquid crystal displays, the small permittivity anisotropy approximation, justified for the magnetic field, is no longer valid. If we take into account the usually significant relative dielectric anisotropy $\gamma = \varepsilon_a/\varepsilon_\perp$, rather complicated expressions for $a_1 \ldots a_6$ are obtained. They have the applicable representation only if $\theta_0 = 0$:

$$\left.\begin{aligned} a_2 &= (\pi^2 k_1/4d)[1 - e - 2k_t(d/\lambda)(\phi/\pi) + (\phi/\pi)^2(k_b - 2k_t)], \\ a_4 &= (\pi^2 k_1/16d)[(k_b - 1) + e(1 + \gamma) + 2k_t(d/\lambda)(\phi/\pi) \\ &\quad + (\phi/\pi)^2(5k_t - 4k_b)], \\ a_6 &= (\pi^2 k_1/144d)[1{\cdot}5(1 - k_b) - e(1 - 4\gamma + 4{\cdot}5\gamma^2) - 2k_t(d/\lambda)(\phi/\pi) \\ &\quad + (\phi/\pi)^2(16k_b - 17k_t)], \end{aligned}\right\} \tag{32}$$

where $e = (E/E_s)^2$ and $E_s = (\pi/d)(k_1/\varepsilon_0\varepsilon_a)^{1/2}$. As a result condition (31), generalized for the electric field, takes the form

$$\phi/\pi \gtrless \{(s - \gamma - 2)(d/\lambda) \pm \{(d/\lambda)^2(s - \gamma - 2)^2 + [s^2 - s(1 + \gamma) + 1 + 2\gamma] \times [s - (d/\lambda)^2 + \gamma/k_t]\}^{1/2}\} \cdot [s^2 - s(1 + \gamma) + 1 + 2\gamma]^{-1}. \tag{33}$$

This inequality is equivalent to the criterion given by Raynes [11].

In figures 7(*b*) and 7(*c*) the results of calculations of ξ_m and ψ_m are exemplified.

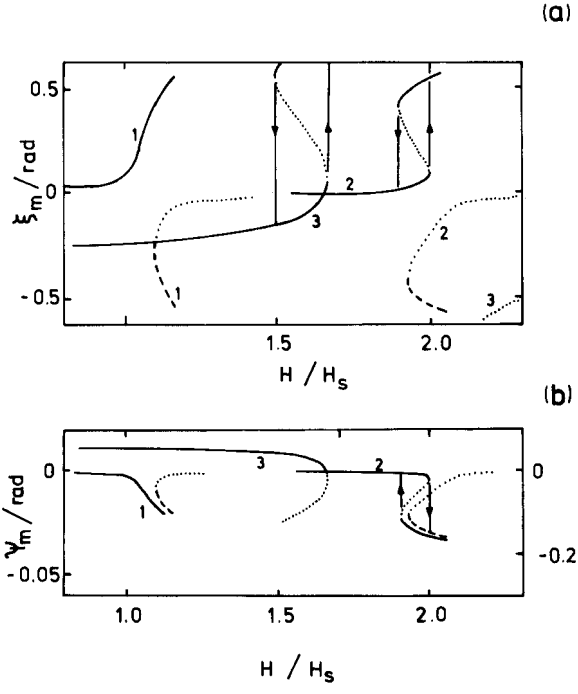

Figure 8. The deformation angles ξ_m (*a*), and ψ_m (*b*) as a function of the reduced field for the pretilted twisted structures. $k_b = 1{\cdot}4$, $k_t = 0{\cdot}4$, $\gamma = 0$. 1: $\phi = \pi/2$, $d/\lambda = 0$, $\theta_0 = 0{\cdot}01$, 2: $\phi = 1{\cdot}5\pi$, $d/\lambda = -1{\cdot}5$, $\theta_0 = 0{\cdot}01$, 3: $\phi = 1{\cdot}5\pi$, $d/\lambda = -1{\cdot}5$, $\theta_0 = 0{\cdot}3$. Curve 1 in (*b*) is described by the left scale, curves 2 and 3 by the right scale.

5.2. $\theta_0 \neq 0$

It is impossible to derive analytical expressions of the type given in equation (31) for $\theta_0 \neq 0$. For this application, the analysis of trajectories in four-dimensional control space is impracticable. Therefore only the plots of the deformation angles are shown in figures 8 (*a*) (*b*). The non-zero tilt cancels the threshold. There is $\xi_m \neq 0$ even in the absence of the field, as shown by Fraser [12]. The criteria (31) or (33) for hysteresis are approximately valid for small tilt.

6. Discussion

All of the problems studied here have been resolved earlier by other authors with the aid of traditional variational methods. The reanalysis of them by means of catastrophe theory gives, above all, a clarity in the recognition of stable solutions and of transitions between them. Liquid crystal layers belong to mechanical systems which obey the delay convention: they remain in their minimum of potential energy until this minimum exists. Application of this rule to the movement of a point on the behaviour surface over the corresponding trajectory yields the useful stability criterion. The theorems of catastrophe theory also determine strictly which terms of the Taylor series are significant.

The qualitative results of the calculations agree generally with that obtained in the original studies. However, some minor differences referred to this discussion can be noticed. The hysteresis shown in figure 4 (*b*) was omitted in [5], and different expressions for the function $\xi_m(H/H_b)$ were obtained in [7] because of the improper truncation of the power series. The expansion of the energy in a series of ξ_m was sometimes used in analogy to the Landau expansion in the neighbourhood of a second order phase transition as in [13] and [14]. Similar results to these presented here were obtained for $\alpha \neq \theta_0$ and $\theta_0 = \pi/2$ in [13].

The energies of the layers considered were calculated by use of an approximation justified only for small distorsions: the angles $\xi(z)$ and $\psi(z)$ were determined by functions of sinusoidal shape (8) and (17). The Taylor expansion and the energy function are equivalent only locally, i.e. sufficiently close to $\xi_m = 0$ and $\psi_m = 0$. Therefore only pairs of small values of ξ_m and ψ_m are acceptable. In particular the predicted range of bistability of supertwisted structures disagrees with data from [11], because the distorsion takes rather high values.

All of the essential features of the director behaviour found here are well-known from numerous experimental studies, e.g. [5], [13], [15], [16] or from applications [17], [18]. Some of the predicted effects seem however to be too subtle to be detected, (for instance the hysteresis shown in figures 5 and 6).

Throughout the paper the positive anisotropies $\chi_a > 0$ or $\varepsilon_a > 0$ were assumed. The opposite sign can also be taken into consideration by use of the reverse sign of the field parameters h or e.

For the homogeneously oriented nematic with an external field applied normal to the boundary plates (or for other analogous geometries), the threshold is predicted. The implication of catastrophe theory is that such layers belong to the structurally unstable systems. It is rather difficult to achieve the threshold behaviour strictly. Any fluctuations of alignment and other imperfections, unavoidable in experimental realizations of such systems, create pretilted layers in an oblique field, for which no threshold exists. Small changes in geometry do not affect this continuous increase of the distorsion of the director field: the system is structurally stable. An apparent

threshold may appear as the trajectories may run extremely close to that for perfect geometry.

References

[1] THOM., R., 1972, *Stabilite Structurelle et Morphogenese* (Benjamin).
[2] POSTON, T., and STEWART, I., 1978, *Catastrophe Theory and its Applications* (Pitman).
[3] THOMPSON, J. M. T., 1982, *Instabilities and Catastrophes in Science and Engineering* (Wiley).
[4] VASILYEV, Y. V., 1983, *Zh. teor. Fiz.*, **53**, 590.
[5] ONNAGAWA, H., and MIYASHITA, K., 1974, *Jap. J. appl. Phys.*, **13**, 1741.
[6] POSTON, T., and STEWART, I., 1976, *Taylor Expansions and Catastrophes* (Pitman).
[7] YAMADA, H., 1984, *Molec. Crystals liq. Crystals*, **108**, 93.
[8] MOTOOKA, T., and FUKUHARA, A., 1979, *J. appl. Phys.*, **50**, 3322.
[9] MATSUMOTO, S., KAWAMOTO, M., and MIZUNOYA, K., 1976, *J. appl. Phys.*, **47**, 3842.
[10] LESLIE, F. M., 1970, *Molec. Crystals liq. Crystals*, **12**, 57.
[11] RAYNES, E. P., 1986, *Molec. Crystals liq. Crystals Lett.*, **4**, 1.
[12] FRASER, C., 1978, *J. Phys.* A, **11**, 1439.
[13] OLDANO, C., MIRALDI, E., and TAVERNA VALABREGA, P., 1984, *J. Phys., Paris*, **45**, 755.
[14] DEULING, H. J., GABAY, M., GUYON, E., and PIERANSKI, P., 1975, *J. Phys.. Paris*, **36**, 689.
[15] MEYERHOFER, D., 1975, *Physics Lett.*, **51A**, 407.
[16] OLDANO, C., MIRALDI, E., STRIGAZZI, A., TAVERNA VALABREGA, P., and TROSSI, L., 1984, *J. Phys., Paris*, **45**, 355.
[17] SCHEFFER, T. J., and NEHRING, J., 1984, *Appl. Phys. Lett.*, **45**, 1021.
[18] SCHADT, M., and LEENHOUTS, F., 1987, *Appl. Phys. Lett.*, **50**, 236.